ChemPubSoc Europe

DOI: 10.1002/slct.201900199

Chemistry SELECT Full Papers

Analytical Chemistry

Cinnamaldehyde-Based Chemosensor for Colorimetric Detection of Cu^{2+} and Hg^{2+} in a Near-Perfect Aqueous Solution

Hanna Cho, Ju Byeong Chae,* and Cheal Kim*[a]

A cinnamaldehyde-based colorimetric chemosensor **TAA** (N′-((1E,2Z)-3-(4-(dimethylamino)phenyl)allylidene)thiophene-2-carbohydrazide) was newly developed. **TAA** can detect Cu^{2+} and Hg^{2+} ions by different color changes from pale yellow to deep yellow and orange, respectively, in aqueous media. **TAA** differently binds to Cu^{2+} as a 1:1 ratio and Hg^{2+} as a 2:1 ratio. The detection limits towards both analytes turned out to be 0.08 μM for Cu^{2+} and 0.01 μM for Hg^{2+}. Moreover, **TAA** could successfully quantify Cu^{2+} and Hg^{2+} in tap and drinking water. The detection processes of **TAA** towards Cu^{2+} and Hg^{2+} were demonstrated by using DFT calculations.

Introduction

Quite recently, a number of detection methods for metal ions have been developed.[1,2] These methods, like stripping voltammetry, atomic absorption spectroscopy and inductively coupled plasma, could detect effectively metal ions, but need skilled operators and complicate procedures.[2–4] On the contrary, colorimetric detection using chemosensors has been known as a cost-effective tool due to easy detection via naked-eye without expensive equipment.[5–7] Thus, it is really needed to develop effective and selective colorimetric chemosensors for metal ions.[8–11]

Detection of copper and mercury has attracted high attention in the field of chemosensors,[12–15] because of their environmental and biological influence. Copper is an essential transition metal in living organisms,[16,17] but the pollution of copper in the atmosphere or soil could have negative effects to them.[18,19] The exposure to high concentrations of copper ions for long periods is known to cause hemolytic anemia, hepatitis and Parkinson's disease.[20–22] Mercury is a well-known toxic transition metal.[23–25] Recent reports highlighted the affection of mercury pollution towards not only soil bacteria and fungi but also human beings.[26–28] Therefore, the development of effective and selective chemosensors for copper and mercury is highly demanded.[29–32]

Many chemosensors for detecting Cu^{2+} or Hg^{2+} have been developed, and some of them show very low detection limits like nanomolar and attomolar concentrations.[11,15,16,22,23,25] On the other hand, chemosensors for detecting both Cu^{2+} and Hg^{2+} by a colorimetric method have been recently developed using several chromophores such as BODIPY,[33–35] pyrene,[36,37] NBD,[38] phenothiazine,[39] rhodamine,[40] and naphthalimide.[41] Nevertheless, they have a limitation for practical application due to the poor solubility in water. Only two examples are soluble in a near-perfect aqueous media. For the practical and efficient usage of chemosensor, it is highly demanded to develop colorimetric chemosensors working in water.[42]

Chemosensors using cinnamaldehyde moiety were applied to detect metal cations because its long conjugation could induce a unique spectral change by binding to metal ions.[43,44] However, the low solubility of the cinnamaldehyde moiety in water was a big obstacle to development of the cinnamaldehyde-based practical chemosensors.[45] For solving this problem, we envisioned to use a thiophene derivative having a hydrazide functional group, which would have a good water-soluble property.[46] Hence, we expected that the combination of cinnamaldehyde and thiophene-2-carbohydrazide would have better water solubility and show a unique spectral change to heavy metal ions.

Herein, we presented a new cinnamaldehyde-based chemosensor **TAA**, which detected Cu^{2+} and Hg^{2+} by color change in a near-perfect aqueous media. Moreover, **TAA** was applied to real water samples for the analysis of Cu^{2+} and Hg^{2+} ions. Possible binding structures and detection processes of **TAA** to Cu^{2+} and Hg^{2+} ions were demonstrated, based on ESI-MS, Job plot and DFT calculations.

Results and Discussion

TAA was given by the reaction of 4-(dimethylamino)cinnamaldehyde and thiophene-2-carbohydrazide (Scheme 1). It was verified with ^{1}H and ^{13}C NMR (Figures S1 and S2), elemental analysis and ESI-MS.

[a] *H. Cho, J. B. Chae, Prof. C. Kim*
Department of Fine Chem., (SNUT) Seoul National Univ. of Sci. and Tech., Seoul 01187, Korea
Tel: +82-2-971-6680
Fax: +82-2-970-9140
E-mail: ch920812@naver.com
chealkim@snut.ac.kr

Supporting information for this article is available on the WWW under https://doi.org/10.1002/slct.201900199

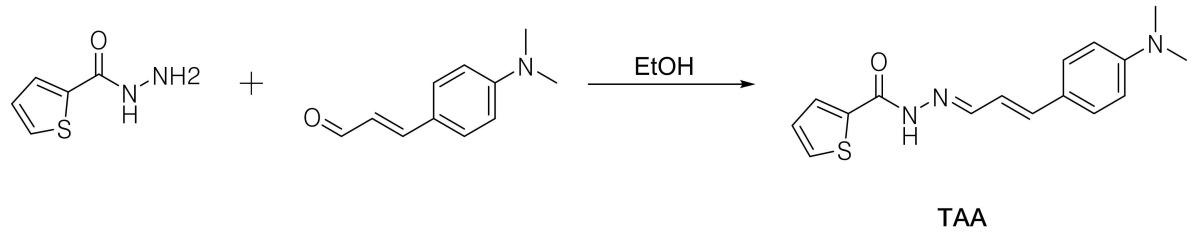

Scheme 1. Synthesis of **TAA**.

Colorimetric detection of Cu^{2+}

Chromogenic selectivity of **TAA** to metal ions with biological and environmental significance was studied in bis-tris buffer (Figure 1). Only Cu^{2+} and Hg^{2+} ions induced remarkable UV-visible change of **TAA** at 480 nm and 518 nm, respectively. The results were consistent with the photograph (Figure 1(b)). **TAA** showed color changes from pale yellow to deep yellow with Cu^{2+} ion and to orange with Hg^{2+} ion. In contrast, spectral and color changes were not observed with other cations. Thus, **TAA** can be a strong candidate of a visible sensor for both Cu^{2+} and Hg^{2+}.

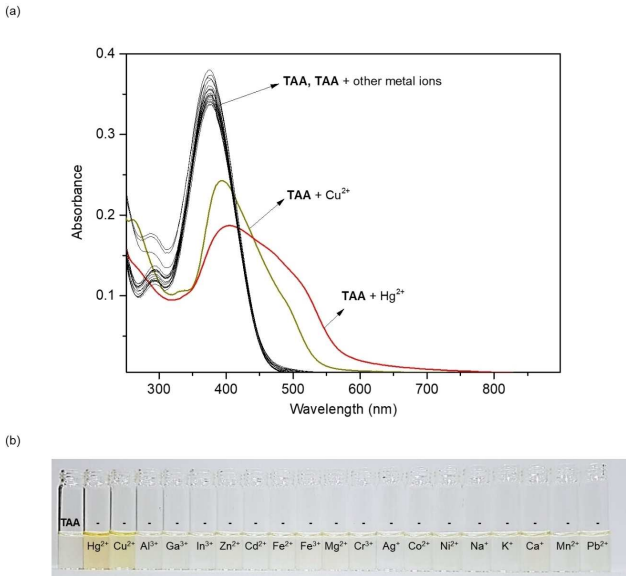

Figure 1. (a) UV-visible changes of **TAA** (10 μM) on addition of diverse cations (2.0 equiv, 20 μM) in bis-tris buffer (pH 7.0, 10 mM). (b) Photograph of **TAA** (10 μM) and **TAA** with diverse cations (2.0 equiv, 20 μM) in bis-tris buffer (pH 7.0, 10 mM).

The binding character of **TAA** with Cu^{2+} ion was checked by UV-visible titration (Figure 2). On the addition of Cu^{2+} ion to **TAA**, the absorption of 380 nm prominently decreased, whereas a novel band at 480 nm consistently increased and reached to a maximum with 2.0 equiv. of Cu^{2+} ion. One isosbestic point

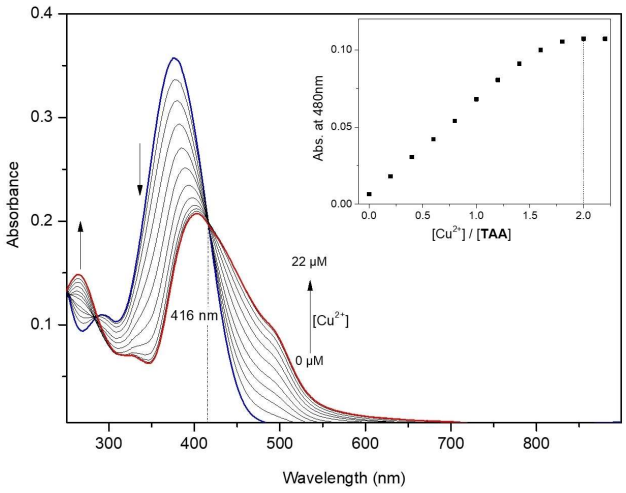

Figure 2. Absorption variations of **TAA** (10 μM) with Cu^{2+} ions (0-2.2 equiv) in bis-tris buffer (pH 7.0, 10 mM). Inset: Plot of the absorbance (480 nm) vs. the amount of Cu^{2+}.

was shown at 416 nm, signifying that a complex was made from **TAA** upon binding with Cu^{2+} ion.

For further understanding of binding mode, we carried out Job plot analysis (Figure S3). The absorbance at 480 nm showed the highest at mole fraction 0.5, which indicates a 1:1 stoichiometry between **TAA** and Cu^{2+}. In addition, the ratio of 1:1 was verified by a positive-ion ESI-MS experiment (Figure 3). In the MS spectrum of **TAA** with 1 equiv. of Cu^{2+}, *m/z* peak at 517.08 could be assigned as $[\mathbf{TAA}\text{-}H^{+} + Cu^{2+}]^{+} + 2\cdot DMSO$, which was well matched with the calculated *m/z* value (517.06). We tried to conduct ^{1}H NMR titration of **TAA** with Cu^{2+} ion, but we could not obtain reliable data owing to paramagnetic property of Cu^{2+} ion. With the results of Job plot and ESI-MS, we envisioned plausible binding structure in Scheme 2. Binding constant (*K*) of $2.9 \times 10^{4}\ M^{-1}$ was given for Cu^{2+}-**TAA** using Li's equation (Figure S4).[47]

The competing selectivity of **TAA** as a chromogenic sensor for the sensing of Cu^{2+} was studied with diverse competing cations (Figure 4). **TAA** was treated with 2.0 equiv. of Cu^{2+} with the same amount of other cations. Most metal ions did not show absorption interference for the sensing of Cu^{2+} ion, except Co^{2+} and K^{+} ions, which interfered with about 20%. Nevertheless, their color change was discernible enough. Thus, **TAA** could be a valuable colorimetric sensor for Cu^{2+} ion with diverse competing cations. We tested the effect of pH on the

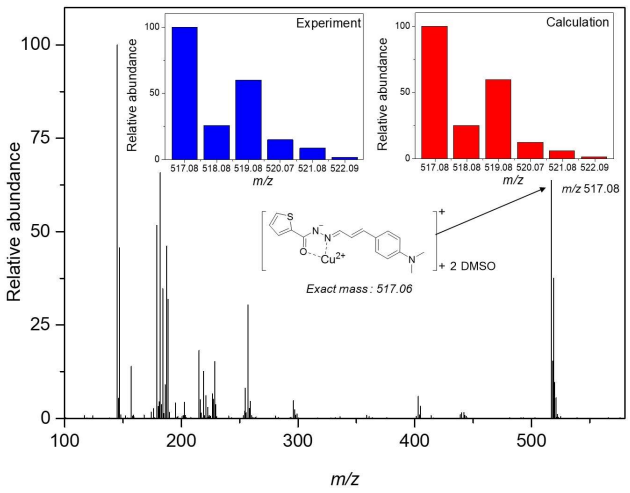

Figure 3. Positive-ion ESI-MS of **TAA** (10 μM) on addition of $Cu(NO_3)_2$.

spectral response of **TAA** to Cu^{2+} in a pH range from 6 to 9 (Figure S5). The remarkable spectral change of Cu^{2+}-**TAA** was observed between pH 6 and 9, suggesting that Cu^{2+} ion can be detected with **TAA** over the environmental pH range of 6–9.

The detection ability of **TAA** towards Cu^{2+} was studied in water samples. With the calibration plot of **TAA** toward Cu^{2+} (Figure 5), each sample was analyzed three times (Table 1).

Table 1. Measurement of Cu^{2+}.[a]

Sample	Cu^{2+} added (μM)	Cu^{2+} found (μM)	Recovery (%)	R.S.D. (n = 3) (%)
Tap water	0.00	0.00	-	-
	3.00	2.90	96.7	0.34
Drinking water	0.00	0.00	-	-
	3.00	2.95	98.3	0.64

[a] Conditions: [**TAA**] = 10 μM in bis-tris buffer.

Reliable recoveries and R.S.D. (relative standard deviation) were given from the water samples. In addition, detection limit (3σ/K) of **TAA** toward Cu^{2+} was given as 0.08 μM (Figure 5), which is much below the WHO protocol (31.4 μM) for Cu^{2+} ion.[48] Surprisingly, the number is the lowest detection limit among those formerly addressed chemosensors for detecting both Cu^{2+} and Hg^{2+} in different colors (Table S1). These consequences demonstrated that **TAA** could be applicable for determination of Cu^{2+} level with an acceptable accuracy and precision.

Colorimetric detection of Hg^{2+}

The binding character of **TAA** to Hg^{2+} ions was checked by UV-visible titration (Figure 6). On the addition of Hg^{2+} to **TAA**, the absorption of 390 nm decreased prominently and a novel broad absorption of 518 nm increased consistently and reached a maximum at 0.5 equiv. of Hg^{2+} ion with the color change from pale yellow to orange. Two defined isosbestic points were formed at 280 and 420 nm, signifying that a species was produced from **TAA** upon binding with Hg^{2+}. The Job plot test afforded a 2:1 ratio of **TAA** to Hg^{2+} (Figure S6). Its result was verified by ESI-MS analysis (Figure S7). The peak of 799.19 (*m/z*) could be assigned as [2·**TAA**-H^+ + Hg^{2+}]$^+$ (calcd *m/z* 799.18).

To understand binding mode, we conducted ^{1}H NMR titration (Figure 7). **TAA** showed a tautomer structure between the amide form (11.68 ppm) and the imidic acid one (11.39 ppm). When 0.5 euqiv of Hg^{2+} was added, the peak (H_4) disappeared. The imine proton H_5 significantly moved to downfield, while the protons on the thiophene and cinnamaldehyde moieties showed small shifts. These results indicated that the carbonyl group and the imine moiety of **TAA** might be involved in binding with Hg^{2+}. With the results of ESI-MS, ^{1}H NMR titration and Job plot, we envisioned the reasonable binding character of Hg^{2+}-2·**TAA** in Scheme 3. Based on the 2:1 ratio, binding constant (*K*) of 2 × 10^9 M^{-2} was given for Hg^{2+}-2·**TAA** using Li's equation (Figure S8).[47]

The competing selectivity of **TAA** as a chromogenic sensor for the sensing of Hg^{2+} was checked with diverse competing cations (Figure 8). **TAA** was treated 0.5 equiv. of Hg^{2+} with the same amount of other cations. There was no prominent interference for the sensing of Hg^{2+} with other cations. Therefore, **TAA** could operate as an outstanding colorimetric probe for Hg^{2+} with diverse competing cations.

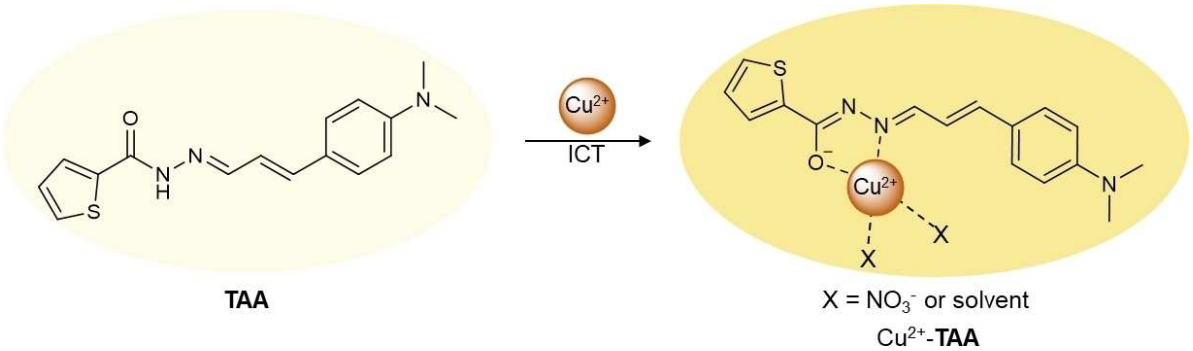

Scheme 2. Plausible binding structure of **TAA** with Cu^{2+} ion.

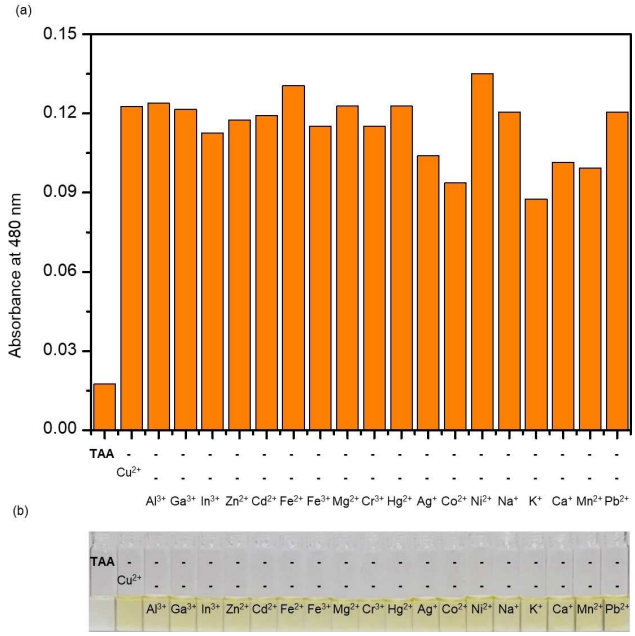

Figure 4. (a) Bar graph (480 nm) for the interaction of **TAA** toward Cu^{2+} and other competing metal ions in bis-tris buffer (pH 7.0, 10 mM). (b) Photograph of **TAA**, Cu^{2+}-**TAA** and Cu^{2+}-**TAA** + other metal ions in bis-tris buffer (pH 7.0, 10 mM).

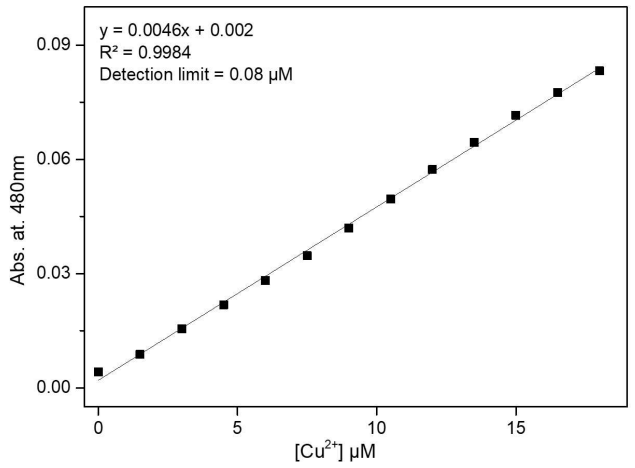

Figure 5. Calibration curve of **TAA** (10 μM) with Cu^{2+} in bis-tris buffer (pH 7.0, 10 mM).

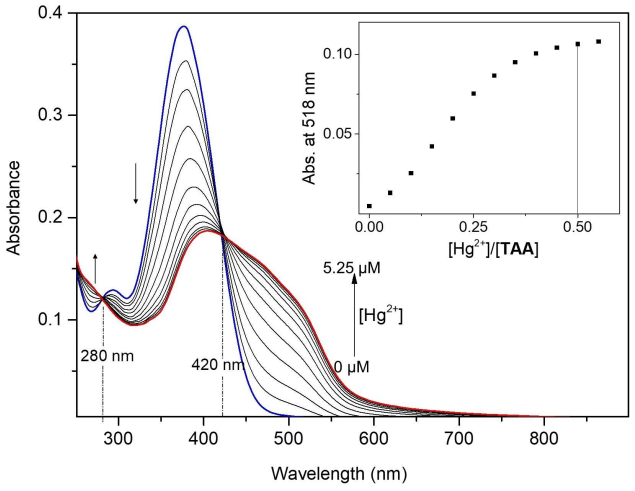

Figure 6. Absorption variations of **TAA** (10 μM) on addition of Hg^{2+} ions (0 - 0.525 euiv) in bis-tris buffer (pH 7.0, 10 mM). Inset: Plots of the absorbance (518 nm) vs. the amount of Hg^{2+}.

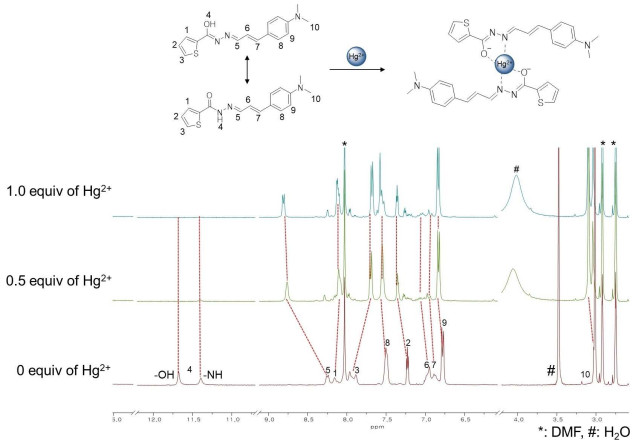

Figure 7. ^{1}H NMR titration of **TAA** with Hg^{2+}.

Table 2. Measurement of Hg^{2+}.[a]

Sample	Hg^{2+} added (μM)	Hg^{2+} found (μM)	Recovery (%)	R.S.D. (n = 3) (%)
Tap water	0.00	0.00	-	-
	1.25	1.27	101.6	1.40
Drinking water	0.00	0.00	-	-
	1.25	1.24	99.2	1.12

[a] Conditions: [**TAA**] = 10 μM in bis-tris buffer.

We tested the effect of pH on the spectral response of **TAA** to Hg^{2+} in pH values of 6 to 9 (Figure S9). The significant absorbance change of Hg^{2+}-2·**TAA** was observed between pH 7 and 9, demonstrating that **TAA** could be applicable for detecting Hg^{2+} over the pH range of 7–9.

Moreover, we conducted real water-sample application using tap and drinking water to examine the feasibility of **TAA** for quantification of Hg^{2+}. The calibration curve was used for calculating R.S.D. and recovery (Figure S10). Reliable R.S.D. and recovery values were afforded (Table 2). The limit of detection (3σ/K) of **TAA** for Hg^{2+} was found out to be 0.01 μM, as low as 0.01 μM regulated by United States Environmental Protection Agency for Hg^{2+}.[49] Therefore, **TAA** could reliably quantify Hg^{2+} in real samples with a low detection limit. Importantly, the detection limit of **TAA** to Hg^{2+} ion was also the lowest among those formerly addressed colorimetric sensors for detecting both Cu^{2+} and Hg^{2+} ions in different colors (Table S1).

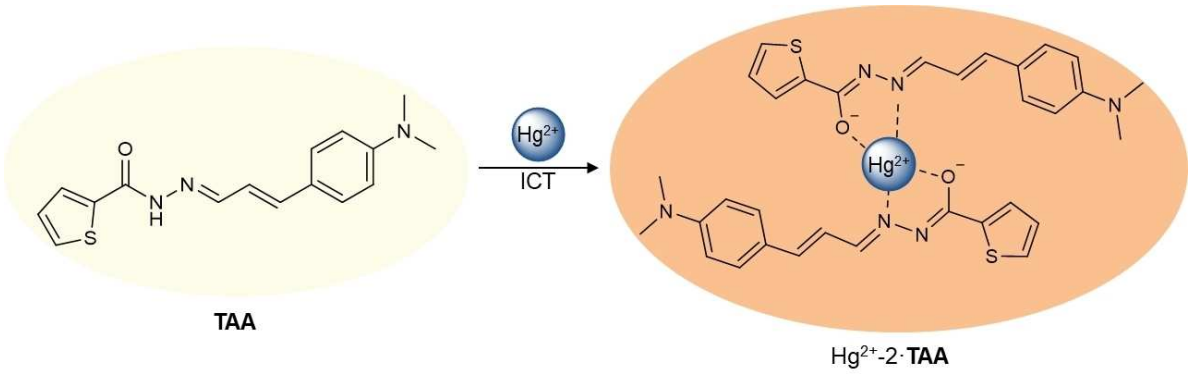

Scheme 3. Plausible binding structure of **TAA** with Hg^{2+}.

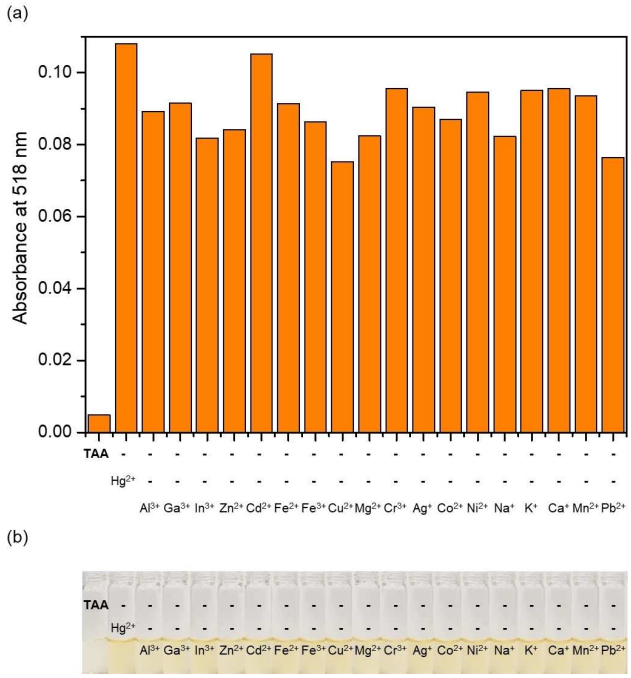

Figure 8. (a) Bar graph (480 nm) for the interaction of **TAA** (10 μM) toward Hg^{2+} and other competing cations (0.5 equiv) in bis-tris buffer (pH 7.0, 10 mM). (b) Photograph of **TAA**, Hg^{2+}-2·**TAA**, and Hg^{2+}-2·**TAA** + other metal ions in bis-tris buffer (pH 7.0, 10 mM).

Theoretical calculations

All calculations were conducted based on the experimental data. The optimized forms of **TAA**, Cu^{2+}-**TAA**, Hg^{2+}-2·**TAA** are presented in Figure 9. The calculated structure of **TAA** was flat with a dihedral angle of 179.99° (1O, 2 C, 3 N, 4 N). The addition of Cu^{2+} and Hg^{2+} ions to **TAA** changed the structure of **TAA** slightly. The dihedral angle of Cu^{2+}-**TAA** complex changed from 179.99° to −2.278°. Hg^{2+}-2·**TAA** showed a tetrahedral structure with a dihedral angle of −6.045°.

By using these optimized structures, we calculated TD-DFT and analyzed possible transitions. **TAA** showed a major absorption at 347.53 nm, which corresponded to intramolecular charge transfer (ICT) from the cinnamaldehyde moiety to the thiophene one (Figures S11 and S13). Cu^{2+}-**TAA** complex showed small ICT and LMCT (Figures S12 and S13). The red-shifted UV-vis spectrum matched the decreased energy gap. In case of Hg^{2+}-2·**TAA**, the major transition appeared at 455.26 nm, which corresponded with ICT (Figures S14 and S15). The second major transition also showed ICT (435.37 nm). Since these transitions might induce larger ICT in Hg^{2+}-2·**TAA** than in Cu^{2+}-**TAA**, different absorption and color changes were observed. Based on experimental and theoretical results, we envisioned the possible structures and sensing mechanisms of Cu^{2+}-**TAA** and Hg^{2+}-2·**TAA** in Schemes 2 and 3.

Conclusions

We presented a cinnamaldehyde-based chemosensor **TAA** for colorimetric sensing of Cu^{2+} and Hg^{2+} ions by different color changes from pale yellow to deep yellow and orange in aqueous media. The detection limits turned out to be 0.08 μM for Cu^{2+} and 0.01 μM for Hg^{2+}, which are the lowest among those previous reported chemosensors for detecting both Cu^{2+} and Hg^{2+} in different colors. For the practical application, **TAA** was well applied to real samples for the analysis of both Cu^{2+} and Hg^{2+}. Based on ESI-MS, Job plot and DFT calculations, different binding structures and sensing mechanisms of Cu^{2+}-**TAA** and Hg^{2+}-2·**TAA** were demonstrated. Therefore, we expected that **TAA** would contribute to designing a new type of cinnamaldehyde-based sensors for detecting metal ions.

Supporting Information Summary

Experimental methods, Job plot analyses, binding constants, detection limits, pH test, ESI-mass spectra, DFT calculations are provided in the supplementary information.

Acknowledgements

The National Research Foundation of Korea (NRF) (2018R1 A2B6001686) was kindly supported for this work.

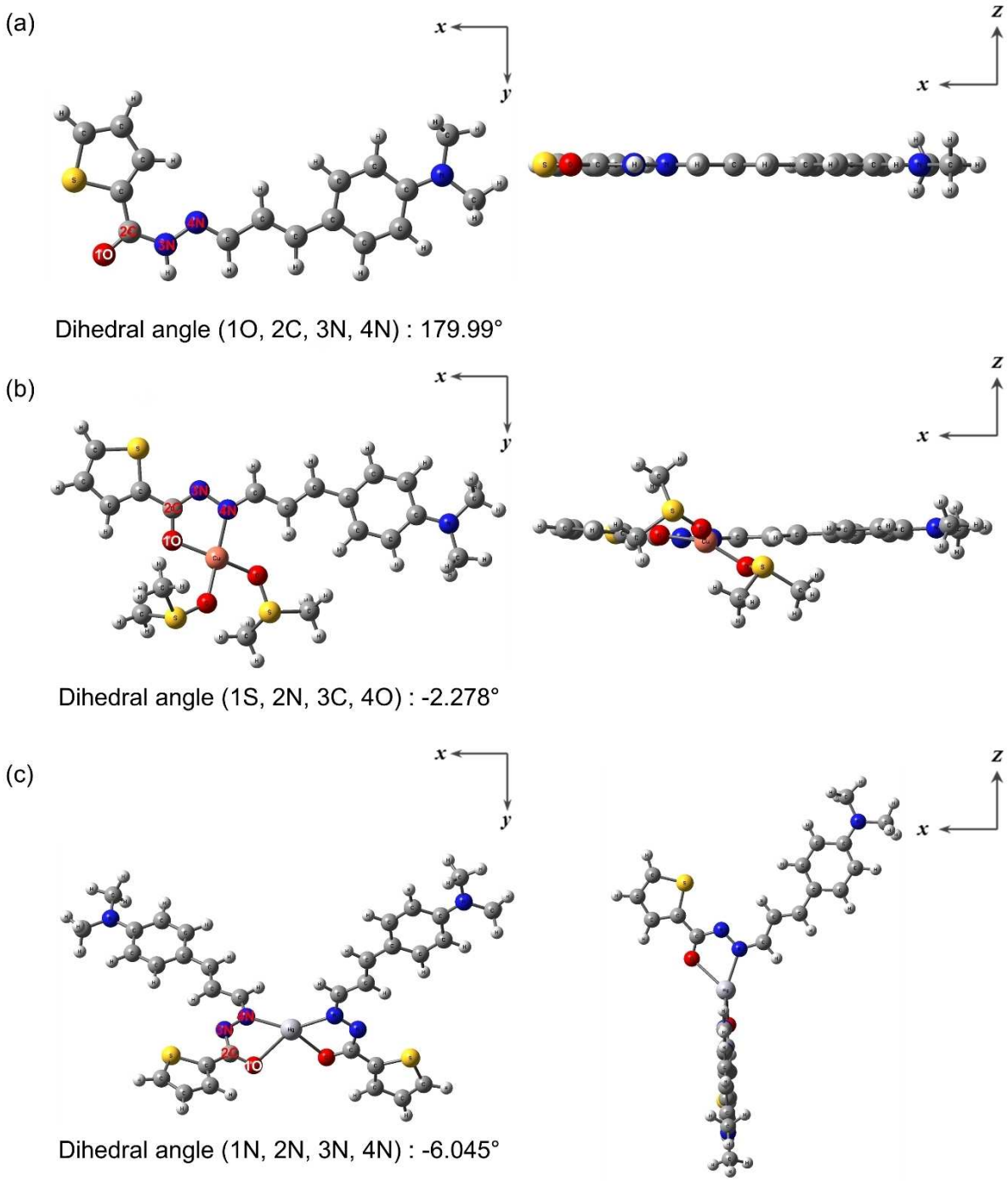

Figure 9. Energy-optimized structures of (a) **TAA**, (b) Cu^{2+}-**TAA**, and (c) Hg^{2+}-2·**TAA**.

Conflict of Interest

The authors declare no conflict of interest.

Keywords: chemosensor · cinnamaldehyde · copper ions · DFT calculations · mercury ions

[1] J.-Z. Ge, Y. Zou, Y.-H. Yan, S. Lin, X.-F. Zhao, Q.-Y. Cao, *J. Photochem. Photobiol. A Chem.* **2016**, *315*, 67–75.
[2] D. Udhayakumari, S. Naha, S. Velmathi, *Anal. Methods.* **2017**, *9*, 552–578.
[3] N. K. Hien, N. C. Bao, N. T. Ai Nhung, N. T. Trung, P. C. Nam, T. Duong, J. S. Kim, D. T. Quang, *Dyes Pigm.* **2015**, *116*, 89–96.
[4] X. Jin, H. Chen, W. Zhang, B. Wang, W. Shen, H. Lu, *Appl. Organomet. Chem.* **2018**, *32*, e4577.
[5] B. Kaur, N. Kaur, S. Kumar, *Coord. Chem. Rev.* **2018**, *358*, 13–69.
[6] H. J. Jang, T. G. Jo, C. Kim, *RSC Adv.* **2017**, *7*, 17650–17659.
[7] D. Xu, L. Tang, M. Tian, P. He, X. Yan, *Tetrahedron Lett.* **2017**, *58*, 3654–3657.

[8] Y. J. Na, Y. W. Choi, J. Y. Yun, K.-M. Park, P.-S. Chang, C. Kim, *Spectrochim. Acta A.* **2015**, *136*, 1649–1657.
[9] T. He, C. Lin, Z. Gu, L. Xu, A. Yang, Y. Liu, H. Fang, H. Qiu, J. Zhang, S. Yin, *Spectrochim. Acta A.* **2016**, *167*, 66–71.
[10] G. R. You, G. J. Park, J. J. Lee, C. Kim, *Dalton Trans.* **2015**, *44*, 9120–9129.
[11] D. Maity, A. K. Manna, D. Karthigeyan, T. K. Kundu, S. K. Pati, T. Govindaraju, *Chem. Eur. J.* **2011**, *17*, 11152–11161.
[12] M. Pannipara, A. G. Al-Sehemi, A. Irfan, M. Assiri, A. Kalam, Y. S. Al-Ammari, *Spectrochim. Acta A.* **2018**, *201*, 54–60.
[13] L. Chang, Q. Gao, S. Liu, C. Hu, W. Zhou, M. Zheng, *Dyes Pigm.* **2018**, *153*, 117–124.
[14] T. Puangsamlee, Y. Tachapermpon, P. Kammalun, K. Sukrat, C. Wainiphithapong, J. Sirirak, N. Wanichacheva, *J. Lumin.* **2018**, *196*, 227–235.
[15] D. Maity, T. Govindaraju, *Chem. Eur. J.* **2011**, *17*, 1410–1414.
[16] D. Maity, D. Karthigeyan, T. K. Kundu, T. Govindaraju, *Sens. Actuators B.* **2013**, *176*, 831–837.
[17] J. Dong, J. Hu, H. Baigude, H. Zhang, *Dalton Trans.* **2018**, *47*, 314–322.
[18] S. M. Hwang, J. B. Chae, C. Kim, *Bull. Korean Chem. Soc.* **2018**, *39*, 925–930.
[19] A. K. Mahapatra, G. Hazra, N. K. Das, S. Goswami, *Sens. Actuators B.* **2011**, *156*, 456–462.
[20] N. Narayanaswamy, T. Govindaraju, *Sens. Actuators B.* **2012**, *161*, 304–310.
[21] S. Goswami, D. Sen, N. K. Das, *Org. Lett.* **2010**, *12*, 856–859.
[22] D. Maity, A. Raj, D. Karthigeyan, T. K. Kundu, T. Govindaraju, *RSC Adv.* **2013**, *3*, 16788–16794.
[23] P. Makam, R. Shilpa, A. E. Kandjani, S. R. Periasamy, Y. M. Sabri, C. Madhu, S. K. Bhargava, T. Govindaraju, *Biosens. Bioelectron.* **2018**, *100*, 556–564.
[24] K. Zhong, X. Zhou, R. Hou, P. Zhou, S. Hou, Y. Bian, G. Zhang, L. Tang, X. Shang, *RSC Adv.* **2014**, *4*, 16612–16617.
[25] M. Pandeeswar, S. P. Senanayak, T. Govindaraju, *ACS Appl. Mater. Interfaces.* **2016**, *8*, 30362–30371.
[26] Y. Gao, C. Zhang, S. Peng, H. Chen, *Sens. Actuators B.* **2017**, *238*, 455–461.
[27] A. K. Müller, K. Westergaard, S. Christensen, S. J. Sørensen, *FEMS Microbiol. Ecol.* **2001**, *36*, 11–19.
[28] M. Ponram, U. Balijapalli, B. Sambath, S. K. Iyer, V. B. R. Cingaram, K. Natesan Sundaramurthy, *New J. Chem.* **2018**, *42*, 8530–8536.
[29] X. He, J. Zhang, X. Liu, L. Dong, D. Li, H. Qiu, S. Yin, *Sens. Actuators B.* **2014**, *192*, 29–35.
[30] L. He, H. Tao, S. Koo, G. Chen, A. Sharma, Y. Chen, I.-T. Lim, Q.-Y. Cao, J. S. Kim, *ACS Appl. Bio Mater.* **2018**, *1*, 871–878.
[31] T. G. Jo, Y. J. Na, J. J. Lee, M. M. Lee, S. Y. Lee, C. Kim, *New J. Chem.* **2015**, *39*, 2580–2587.
[32] S. Bayindir, *J. Photochem. Photobiol. A Chem.* **2019**, *372*, 235–244.
[33] X. He, J. Zhang, X. Liu, L. Dong, D. Li, H. Qiu, S. Yin, *Sens. Actuators B.* **2014**, *192*, 29–35.
[34] W. J. Shi, J. Y. Liu, D. K. P. Ng, *Chem. Asian. J.* **2012**, *7*, 196–200.
[35] J. Huang, X. Ma, B. Liu, L. Cai, Q. Li, Y. Zhang, K. Jiang, S. Yin, *J. Lumin.* **2013**, *141*, 130–136.
[36] W.-C. Lin, C.-Y. Wu, Z.-H. Liu, C.-Y. Lin, Y.-P. Yen, *Talanta.* **2010**, *81*, 1209–1215.
[37] R. Martínez, A. Espinosa, A. Tárraga, P. Molina, *Org. Lett.* **2005**, *7*, 5869–5872.
[38] J. Park, B. In, L. N. Neupane, K.-H. Lee, *Analyst.* **2015**, *140*, 744–749.
[39] M. Kaur, M. J. Cho, D. H. Choi, *Dyes Pigm.* **2016**, *125*, 1–7.
[40] M. Wang, F. Yan, Y. Zou, L. Chen, N. Yang, X. Zhou, *Sens. Actuators B.* **2014**, *192*, 512–521.
[41] H. Mu, R. Gong, Q. Ma, Y. Sun, E. Fu, *Tetrahedron Lett.* **2007**, *48*, 5525–5529.
[42] S. Manna, P. Karmakar, K. Maiti, S. S. Ali, D. Mandal, A. K. Mahapatra, *J. Photochem. Photobiol. A Chem.* **2017**, *343*, 7–16.
[43] S. Y. Lee, J. J. Lee, K. H. Bok, J. A. Kim, Y. K. So, C. Kim, *Inorg. Chem. Commun.* **2016**, *70*, 147–152.
[44] J. M. Jung, C. Kim, R. G. Harrison, *Sens. Actuators B.* **2018**, *255*, 2756–2763.
[45] D. Peralta-Domínguez, M. Rodríguez, G. Ramos-Ortíz, J. L. Maldonado, M. A. Meneses-Nava, O. Barbosa-García, R. Santillan, N. Farfán, *Sens. Actuators B.* **2015**, *207*, 511–517.
[46] F. E. Anderson, J. M. Prausnitz, *Fluid Phase Equilib.* **1986**, *32*, 63–76.
[47] R. Yang, K. Li, K. Wang, F. Zhao, N. Li, F. Liu, *Anal. Chem.* **2003**, *75*, 612–621.
[48] World Health Organization. Office of Library and Health Literature Services. (1988). Styles for bibliographic citations: guidelines for WHO-produced bibliographies, 2nd ed. Geneva: World Health Organization. http://www.who.int/iris/handle/10665/62429.
[49] U. S. EPA (Environmental Protection Agency), *EPA 810/K-92-001.* **1992**,. https://www.epa.gov/dwstandardsregulations/secondary-drinking-water-standards-guidance-nuisance-chemicals#table-of-secondary.

Submitted: January 18, 2019
Accepted: February 19, 2019